Functional Faceted Silver Nano-Hexapods: Synthesis, Structure Characterizations, and Optical Properties

Xiaohua Liu, Rui Huang, and Jing Zhu*

Beijing National Center for Electron Microscopy, Tsinghua University, Beijing 100084, China, and Laboratory of Advanced Materials, Department of Materials Science and Engineering, Tsinghua University, Beijing 100084, China

Received August 30, 2007. Revised Manuscript Received October 5, 2007

We report a new application of the polyol process to produce silver nanohexapods (AgNHs) with a well-defined concave shape and a unique crystal structure. The structure was studied using X-ray diffraction (XRD), scanning electron microscopy (SEM), selected-area electron diffraction (SAED), and high-resolution electron microscopy (HREM). The experimental results were compared with simulations. The AgNHs are single crystals with a face-centered-cubic (FCC) lattice with a lattice constant of 9.6193 Å, larger than the 4.0862 Å of bulk FCC-Ag. Each AgNH has six branches along the ⟨100⟩ directions. Each of these branches terminates with a square-pyramidal tip of four {111} faces. The faceted AgNHs have a skeleton of Ag_6 octahedra stabilized by organic capping molecules. The AgNHs are metastable and decay under electron beam irradiation to FCC-Ag polycrystalline nanoparticles with abundant stacking faults. The AgNHs were found to be a good substrate for chemical sensing using the surface-enhanced Raman scattering (SERS) method.

Introduction

Well-defined metallic nanocrystals with sharp tips, corners, and edges have attracted much attention recently because their properties are strongly dependent on their shapes and sizes,[1–11] for example, important applications such as biological and chemical sensing.[1,6,8–13] Recently, star-shaped gold nanoparticles with sharp tips were synthesized and found to have unique scattering behavior. However, their synthesis involves a complex low yield seeding process.[3,9,12] Most synthetic routes use the polyol process, where organic molecules are used to regulate crystal growth. So far, many papers have studied Ag nanostructure synthesis but focus on convex particle production.[2,13] Synthesis of concave well-defined polyhedral nanocrystals remains a challenge because it involves kinetically controlled growth processes.[14] Herein, we report the synthesis of concave Ag nano-hexapods (AgNHs) and their use as substrates for surface-enhanced Raman scattering (SERS). A bicontinuous structure model is also proposed for these novel nanoparticles based on diffraction experiments and structure simulations.

Experimental Section

Reagents. The following reagents were used as purchased without further purification: $AgNO_3$ (analytical reagent), poly(vinylpyrrolidone) (PVP, MW ∼ 30 000), and ethylene glycol (EG, analytical reagent).

Synthesis. To synthesize the AgNHs, we used a modified polyol process first developed by Sun and Xia.[2,15] For a typical synthesis of AgNHs, 0.48 g of $AgNO_3$ and 0.48 g of PVP were dissolved separately in 15 mL of EG each that served as both a solvent and a reductant. The two solutions were both immediately subjected to vigorous stirring at room temperature (∼25 °C) with magnetic blenders. The $AgNO_3$/EG solution gradually turned brown during stirring, indicating that some Ag nanoparticles had formed by this time. The PVP/EG solution remained clear and colorless. A round-bottom flask containing 15 mL of EG was heated also with vigorous stirring. The temperature was maintained at ∼158 °C by employing a temperature-feedback heating system. Then the $AgNO_3$/EG and PVP/EG solutions were injected into the hot EG simultaneously. The colorless EG solution suddenly turned bright yellow. In contrast to slow dropwise addition of the reactants reported elsewhere,[15] our injection rate was quite fast. Despite the vigorous stirring during the injection process, the temperature of the mixture decreased to ∼120 °C. Following injection, the temperature gradually returned to ∼158 °C in ∼30 min. The reactant mixture was kept at this

* Corresponding author. E-mail: jzhu@mail.tsinghua.edu.cn.

(1) Tian, N.; Zhou, Z. Y.; Sun, S. G.; Ding, Y.; Wang, Z. L. *Science* **2007**, *316*, 732–735.
(2) Sun, Y. G.; Xia, Y. N. *Science* **2002**, *298*, 2176–2179.
(3) Hao, E.; Bailey, R. C.; Schatz, G. C.; Hupp, J. T.; Li, S. Y. *Nano Lett.* **2004**, *4*, 327–330.
(4) Milliron, D. J.; Hughes, S. M.; Cui, Y.; Manna, L.; Li, J. B.; Wang, L. W.; Alivisatos, A. P. *Nature (London)* **2004**, *430*, 190–195.
(5) Wiley, B.; Sun, Y. G.; Chen, J. Y.; Cang, H.; Li, Z. Y.; Li, X. D.; Xia, Y. N. *MRS Bull.* **2005**, *30*, 356–361.
(6) Xia, Y. N.; Halas, N. J. *MRS Bull.* **2005**, *30*, 338–344.
(7) Yin, Y.; Alivisatos, A. P. *Nature (London)* **2005**, *437*, 664–670.
(8) Zhang, J. G.; Gao, Y.; Alvarez-Puebla, R. A.; Buriak, J. M.; Fenniri, H. *Adv. Mater.* **2006**, *18*, 3233–3237.
(9) Hao, F.; Nehl, C. L.; Hafner, J. H.; Nordlander, P. *Nano Lett.* **2007**, *7*, 729–732.
(10) Kim, F.; Connor, S.; Song, H.; Kuykendall, T.; Yang, P. D. *Angew. Chem., Int. Ed.* **2004**, *43*, 3673–3677.
(11) Li, C. C.; Shuford, K. L.; Park, Q. H.; Cai, W. P.; Li, Y.; Lee, E. J.; Cho, S. O. *Angew. Chem., Int. Ed.* **2007**, *46*, 3264–3268.
(12) Nehl, C. L.; Liao, H. W.; Hafner, J. H. *Nano Lett.* **2006**, *6*, 683–688.
(13) Tao, A.; Sinsermsuksakul, P.; Yang, P. D. *Angew. Chem., Int. Ed.* **2006**, *45*, 4597–4601.
(14) Zettsu, N.; McLellan, J. M.; Wiley, B.; Yin, Y. D.; Li, Z. Y.; Xia, Y. N. *Angew. Chem., Int. Ed.* **2006**, *45*, 1288–1292.
(15) Sun, Y. G.; Yin, Y. D.; Mayers, B. T.; Herricks, T.; Xia, Y. N. *Chem. Mater.* **2002**, *14*, 4736–4745.

10.1021/cm702480a CCC: $40.75
Published on Web 12/11/2007

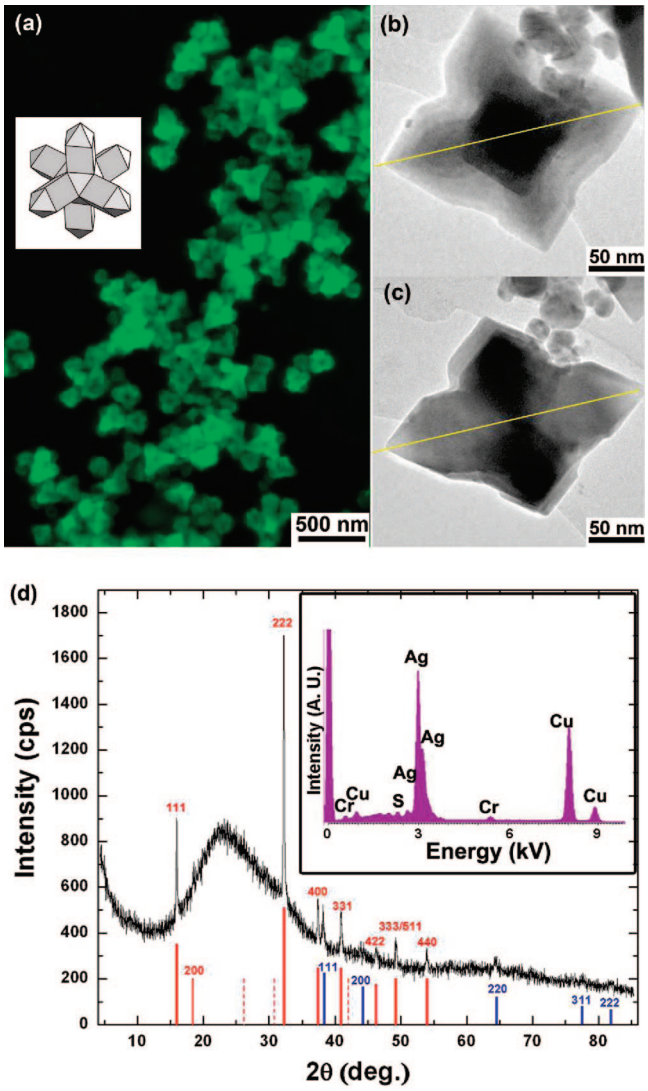

Figure 1. SEM and TEM images of the AgNHs. (a) A typical SEM image shows that most AgNHs stand on the flat substrate with three adjacent tips making contact. The inset is the ideal shape viewed at this orientation. (b, c) Different profiles of an identical AgNH viewed by tilting the sample in the TEM. The yellow lines indicate the rotating axis. (d) XRD spectrum from the AgNHs. Using FCC-Ag as a reference (blue lines), the AgNHs are indexed to an FCC lattice with a constant of 9.6193 Å (red lines). The inset is the EDX spectrum from the AgNH shown in (b) and (c).

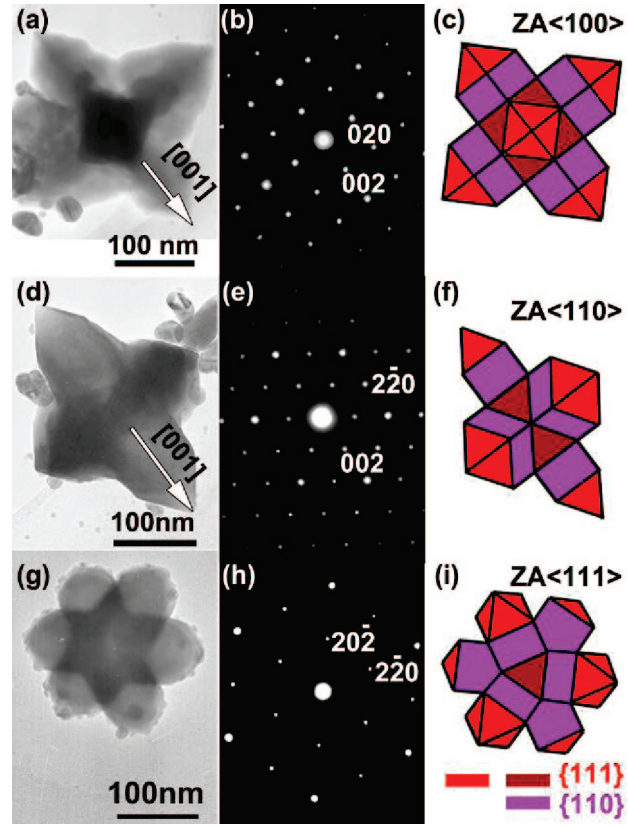

Figure 2. Crystallographic characterizations of the single-crystalline AgNHs by electron microscopy along the three low-index zone axes (ZA): (a–c) ZA ⟨100⟩, (d–f) ZA ⟨110⟩, and (g–i) ZA ⟨111⟩. For each ZA, the TEM images (the left column), the SAED patterns (the medium column), and the surface configurations (the right column) are presented. Each AgNH has six branches along the ⟨100⟩ directions. The tip of each pod is a sharp pyramid of four {111} planes. The lateral surfaces of each pod are {110} planes. The SAED patterns correspond to the identical FCC lattice as the XRD spectrum.

fixed temperature of ∼158 °C for 10 h with stirring. The mixture remained a clear bright yellow. The mixture was sampled at various reaction times, 5 min, 1 h, 2 h, 3 h, and 10 h after mixing. We found that the AgNHs with a well-defined shape had formed after just 5 min. The appearance of the products did not change much with longer reaction times. This indicates that the AgNHs formed quite fast in the injection process and had nearly stopped growing soon after injection. The yield of AgNHs was nearly 100%. This very high yield meant that no subsequent purification was needed for further characterizations.

Characterizations. The as-synthesized AgNHs were rinsed and dispersed into ethanol. The AgNHs were characterized by SEM (JEOL JSM-6301F or Hitachi S5500, operated at 1–5 kV), TEM (JEOL JEM-2010F, 200 kV), XRD (Riguku D/max-RB, wavelength 1.5418 Å), UV–vis spectroscopy (Punkinje General TU-1901), and Raman spectroscopy (Renishaw RM-2000, argon laser, wavelength 514 nm). The AgNHs/ethanol suspension was dropped onto a clean silicon wafer, a carbon-coated copper grid, and a glass slide for SEM, TEM, and XRD characterization, respectively. The UV–vis spectrum was taken from a AgNHs/ethanol suspension. For SERS experiments, one drop of R6G aqueous solution (10^{-6} mol/L, ∼50 μL) was dropped onto the AgNHs supported by a glass slide (1 cm × 3 cm). After the evaporation of the solvent, the sample was exposed to a green Ar-laser (objective lens 50×, acquisition time 30 s, cumulate 5 times).

Results and Discussion

Crystallographic Analysis. Figure 1a shows SEM image of AgNHs sitting on a flat silicone wafer appearing starlike with six sharp tips. Figure 1b,c shows TEM images of a particular AgNH viewed from different angles. The tip-to-tip length is typically 250 nm. Figure 1d shows the XRD and energy dispersive X-ray (EDX) spectra of the AgNHs dispersed on a glass slide. With time the AgNHs decay to FCC silver nanoparticles. This is why diffraction peaks from both FCC-Ag and AgNHs appear in the XRD spectrum. Using FCC-Ag as a reference, the AgNHs were confirmed to also be FCC, but with a larger lattice constant of 9.6193 Å. This is significantly larger than bulk FCC-Ag (JCPDS No. 04-783, $a_{\text{FCC-Ag}} = 4.0862$ Å). The broad peak centered at $2\theta = 23°$ arises from the amorphous glass slide. The {111} and {222} peaks are more intense than expected due to the preferential orientation of the ⟨111⟩ directions perpendicular to the surface of the glass slide. The EDX spectrum from

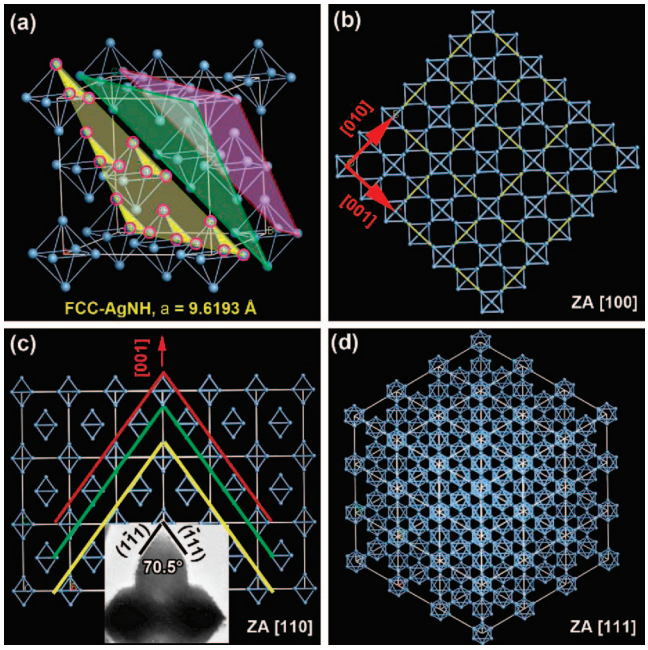

Figure 3. Bicontinuous structure model of the AgNHs derived from the XRD and SAED experiments. (a) The skeleton composed of Ag_6 octahedra in the unit cell with the FCC lattice. The lattice constant is 9.6193 Å. The Ag–Ag bond length in the Ag_6 octahedra is 2.884 Å. The Ag skeleton should be stabilized by capping molecules as the Ag atoms are not close-packed, as indicated by the red circles in the yellow {111} plane. The green {111} plane is closer to the adjacent purple plane than to the yellow plane, resulting in a lower coordination number of 4 for each Ag atom in the lattice. The capping molecules are not shown. (b) The projected image of 3 × 3 × 3 unit cells along ZA [100]. It shows a bicontinuous structure, i.e., both the Ag skeleton and the channel form three-dimensional (3D) networks along the ⟨100⟩ direction. The capping molecules (PVP in our experiments) are most probably located in the straight channel to stabilize the Ag skeleton. (c) The projected image along ZA [110]. The purple, green, and yellow lines correspond to the purple, green, and yellow {111} planes shown in (a). The inset TEM image shows a pyramidal tip defined by four {111} planes. At this visual angle, the shape of the tip exhibits the angle of 70.5° corresponding to the two opposite {111} planes. (d) The projected image along ZA [111].

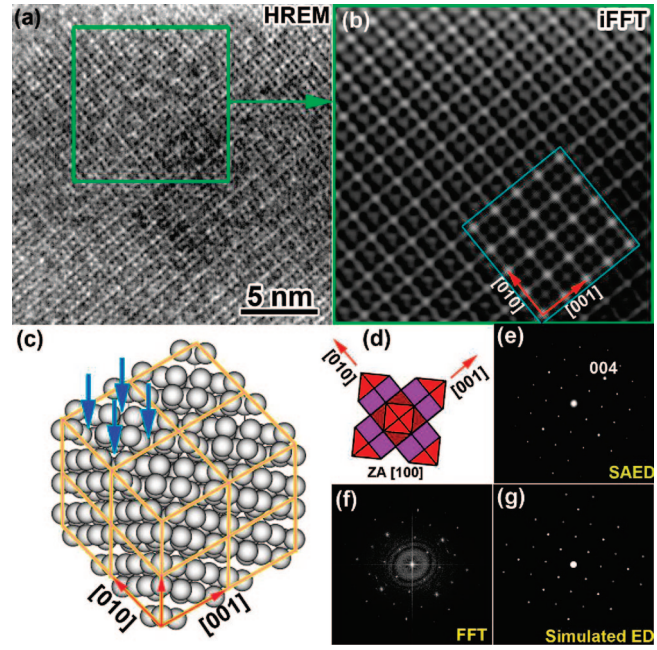

Figure 4. Comparison between the experimental HREM image, the SAED pattern, and simulations. (a) Experimental HREM image with ZA [100]. (b) iFFT image from the green box in (a) with simulated HREM image embedded (blue box). The red arrows indicate two axes of the unit cell. (c) Skeleton made of Ag_6 octahedra. The blue arrows indicate four adjacent channels along the [100] direction. (d) Appearance of the AgNH down the ZA [100]. (e) Experimental SAED pattern. (f) FFT pattern from the experimental HREM image (a). The rings are from the amorphous carbon film supporting the sample. (g) Simulated SAED pattern.

Table 1. Structure Factors of the (*hkl*) Planes for the Kinematical Electron Diffraction

(*hkl*)	phase of F_{hkl}	$\lvert F_{hkl}\rvert$ (nm)
200	0	9.868
400[a]	0	15.728
600	0	7.732
220	π	5.982
440[a]	0	9.504
660	0	2.046
111	0	6.520
222[a]	π	18.158
333	π	9.495
420	0	3.830
422	π	6.096
444	0	6.147

[a] These planes have unusual large electron diffraction intensity.

the individual AgNH in Figure 1b shows strong Ag peaks as expected. Some additional small peaks exist including copper from the TEM grid, chromium from the TEM chamber, and sulfur due to the partial sulfidation of the AgNHs. With exposure to the open air, the AgNHs gradually react to form sulfides similar to other silver nanostructures reported previously.[16]

The SAED patterns (Figure 2b,e,h) show the AgNHs are single crystals. Using the SAED data alongside the TEM images, the surface configuration of the AgNHs was determined (Figure 2). Each AgNH has six identical branches along equivalent ⟨100⟩ directions. Each terminates with a sharp pyramidal tip of four {111} faces. The sides of each branch is enclosed by four equivalent planes of approximately {110}. However, the base of each arm is slightly thicker than the tip, implying some very slow lateral growth accompanied the tip's fast elongation. This is consistent with the higher surface energy of the {110} planes in a FCC crystals.[17] The growth planes for each tip should be the four {111} planes, which form a growth direction along the ⟨100⟩ directions.

For isotropic FCC Ag crystals the equilibrium shape should be a convex polyhedron enclosed by {111} and {100} planes.[17] The concave hexapod shape then is certainly not the equilibrium one. Thus, the growth of the AgNHs must be kinetically rather than thermodynamically controlled. This is consistent with the fast growth during our synthesis, in contrast with the relatively slow growth rate of convex nanoparticles formed by a similar polyol approach using longer reaction times.[15]

Bicontinuous Structure Model. As the scattering factors of electrons by heavy elements are much larger than those of light elements such as hydrogen, carbon, or oxygen, then

(16) Elechiguerra, J. L.; Larios-Lopez, L.; Liu, C.; Garcia-Gutierrez, D.; Camacho-Bragado, A.; Yacaman, M. J. *Chem. Mater.* **2005**, *17*, 6042–6052.

(17) Frenken, J. W. M.; Stoltze, P. *Phys. Rev. Lett.* **1999**, *82*, 3500–3503.

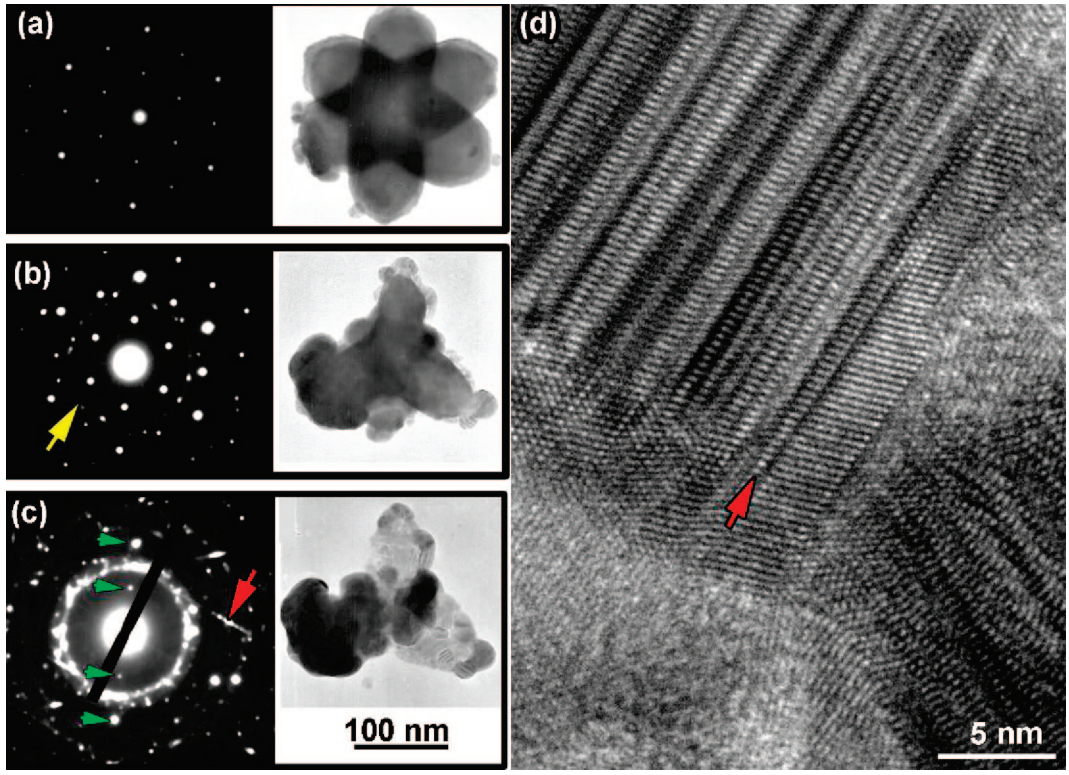

Figure 5. Metastability of the AgNH under electron beam irradiation. (a) Before irradiation, the AgNH is single-crystalline, as indicated by the SAED pattern (left) and the well-defined shape in the TEM image (right). (b) In the process of irradiation, the FCC-Ag {111} ring (marked by the yellow arrow) appears in the SAED pattern. (c) After irradiation. The green arrows indicate the diffraction spots from remnant core of the AgNH. (d) HREM image of the FCC-Ag crystallite with abundant stacking faults, consistent with the diffraction pattern indicated by the red arrow in the SAED pattern in (c). This also agrees with the layered structure of the {111} planes shown in Figures 3 and 4c. By removing the capping molecules, the Ag skeleton collapse to FCC-Ag with abundant stacking faults.

from the EDX we know that the AgNHs are mainly composed of silver. The silver atom positions in the AgNH can be identified using X-ray and electron diffraction combined with simulations. The AgNHs are composed of Ag_6 octahedra (Figure 3). These octahedra form an FCC Braivas lattice with 24 Ag atoms in each unit cell (space group *Fm*3*m*). The coordinates of the Ag atoms in the lattice are (0.212, 0, 0) and equivalent positions. The Ag–Ag distance in the Ag_6 octahedra is 2.884 Å, identical to that in bulk FCC-Ag.

In bulk FCC-Ag the coordination number (CN) is 12; however, in the AgNHs structure the CN is only 4. The purple and green planes in Figure 3a show the outer surfaces of a close-packed layer of Ag_6 octahedra. The thickness of this close packed layer is less than the separation of close-packed layers (distance between green and yellow planes).

The Ag skeleton is a bicontinuous structure, as shown in the [100] projection (Figure 3b). There are three-dimensionally (3D) continuous channels through the Ag_6 octahedra network along all the ⟨100⟩ directions. These channels connect all the tetrahedral interstices of the FCC-AgNH lattice into a cubic network, in which capping molecules are most probably located. Capping molecules must be present in order to stabilize this low CN structure. This is also consistent with previous reports that PVP molecules selectively interact with Ag {100} planes.[5] Parts c and d of Figure 3 show the projected image along ZA [110] and [111], respectively. The tip is defined by four {111} planes, meeting at 70.5° viewed along ZA [110]. The bicontinuous structure is similar to the isoreticular metal–organic frameworks (MOFs), in which metal clusters were linked by organic molecules.[18,19] But in our model the polymer molecules (PVP) with much higher molecular weight seem likely to occupy the channels.

The packing density of the Ag atoms in the FCC-AgNH lattice, ξ, can be calculated as follows:

$$\zeta = \frac{N(4\pi {r_{\mathrm{Ag}}}^3/3)}{{a_{\mathrm{FCC\text{-}AgNH}}}^3} \quad (1)$$

Here $N = 24$ is the number of Ag atoms per unit cell; r_{Ag} is the Ag atom radius (1.442 Å as half-of the Ag–Ag bond length in the Ag_6 octahedron). The calculated ξ_{AgNH} is 0.34, while the ξ for FCC-Ag is 0.74, allowing plenty of room for capping molecules.

HREM Simulations. Figure 4 compares the experimental HREM image and SAED pattern with simulations. The experimental HREM image in Figure 4a was filtered by inverse fast Fourier transform (iFFT) for clarity. The iFFT HREM image within the green box is enlarged and shown in Figure 4b. The blue box is a simulated HREM image using the multislice method in the EMS program.[20] The parameters for the HREM simulation were sample thickness $t = 1.92$ nm, slice thickness $t_s = 0.241$ nm, spherical aberration coefficient of the

(18) Hollingsworth, M. D. *Science* **2002**, *295*, 2410–2413.
(19) Eddaoudi, M.; Kim, J.; Rosi, N.; Vodak, D.; Wachter, J.; O'Keefe, M.; Yaghi, O. M. *Science* **2002**, *295*, 469–472.
(20) Stadelmann, P. A. *Ultramicroscopy* **1987**, *21*, 131–145.

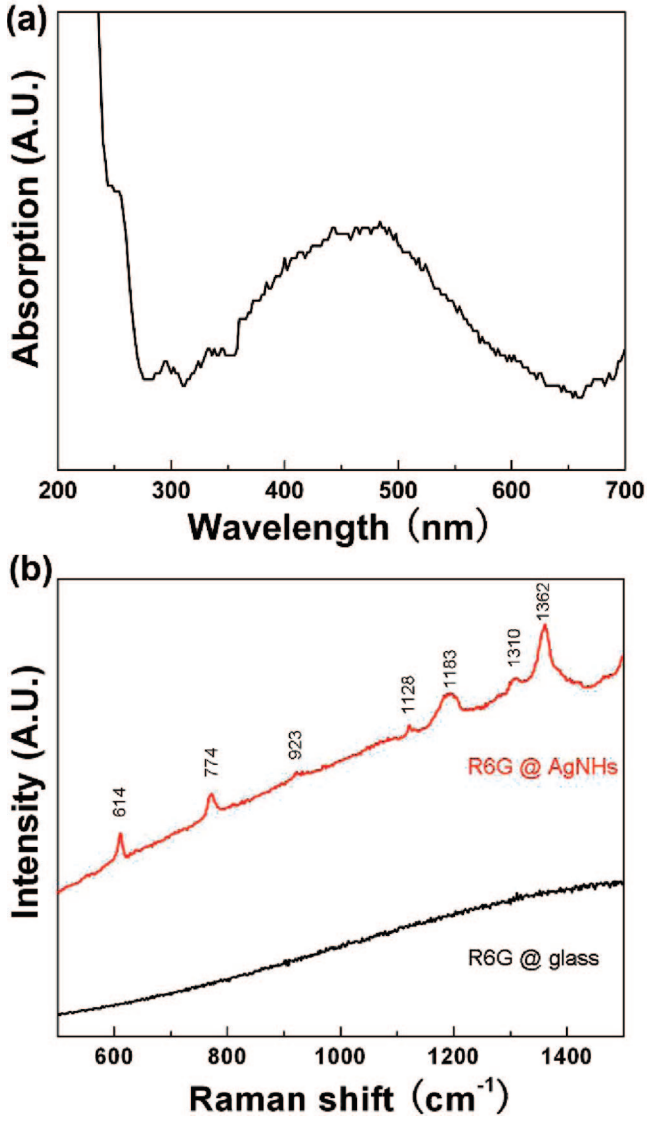

Figure 6. Optical properties of the AgNHs. (a) UV–vis spectrum of the AgNHs dispersed in ethanol. There are fine features in the broad peak appearing in the wavelength range of 300–600 nm, indicating multiple SPR modes as a result of the concave shape of the AgNHs. (b) SERS efficiency of the AgNHs as chemical sensing agents. The spectrum from the sample free from AgNHs displays no features (lower), whereas the other from the AgNHs substrate shows clear characteristic peaks from the probing molecule (R6G).

objective lens of the TEM (JEOL 2010F) $C_s = 0.958$ mm, defocus $\Delta f = -40$ nm, spread of the focus $\Delta = 10$ nm, Debye–Waller factor of silver DWF = 0.004, and the convergence angle $\alpha = 0.1$ mrad. For the simulation we placed a carbon atom in the center of each tetrahedral interstice of the FCC-AgNH lattice to approximate the organic molecules in the channels. Carbon was chosen because it has a medium atomic number among the light elements (hydrogen, carbon, nitrogen, and oxygen) of the molecules. The carbon chains lie along the ⟨100⟩ directions, indicated by the blue arrows in Figure 4c. The interaction of the capping molecules with the Ag_6 octahedra is presently unclear, and the exact location of these molecules is unknown and still under investigation. This may explain why the HREM image features (Figure 4a) are less clear than simulated (inset of Figure 4b).

SAED Simulations. As the atomic number of silver (47) is much larger than those of the elements in the organic molecules, the scattering from these molecules can be neglected. The structure factors of some low-index (*hkl*) planes for the kinematical electron diffraction, F_{hkl}, are calculated using eq 2 and shown in Table 1:

$$F_{hkl} = \sum_{j-l}^{24} f_j \exp[2\pi i(hx_j + ky_j + lz_j)] \quad (2)$$

The atomic scattering factor, f_j, is obtained as the interpolated value of the data listed in Hirsh's classical book.[21] Figure 4e shows the experimental SAED pattern, Figure 4f shows the FFT pattern from the experimental HREM image, and Figure 4g shows the simulated SAED pattern.[20] Within the kinematical approximation $|F_{hkl}|^2$ is proportional to the intensity of the diffraction spots in the electron diffraction pattern. The simulated SAED pattern agrees well with the FFT pattern, whereas it shows some discrepancy with the experimental SAED pattern (Figure 4e). This may arise from the dynamic nature of the experimental conditions of the SAED test. The FFT pattern from the experimental HREM image gives more localized information than from the SAED pattern. The {*hhh*} diffraction peaks in the XRD spectrum (Figure 1d) are stronger than the calculated results from the Materials Studio program (not shown), consistent with the preferential orientation as shown in Figures 1a and 2g. The {400}, {440}, and {222} spots in the SAED patterns are stronger (Figure 2b,e,h), consistent with the larger norms of their structure factors (Table 1).

Metastability. The bicontinuous structure, and hence the whole AgNH, becomes metastable upon removal of the organic molecules and begins to decay. This indicates the bonding between Ag atoms and capping molecules is weak. The AgNHs collapse faster under electron beam irradiation (Figure 5). The AgNHs are relatively stable under electron beam irradiation of very low intensity. This decay is significantly accelerated on increasing beam intensity over 90 pA/cm^2 (as indicated by the sensor on the JEOL 2010 TEM at the magnification of 300 000×). Extensive investigations reveal that the protruding branches, which do not contact the TEM grid, tend to collapse faster. The SAED pattern changes to FCC-Ag rings accordingly (Figure 5a–c). This decomposition may be due to the breaking of weak bonds by either the knocking off or heating effect of the electron beam. With the formation of conducting FCC-Ag decomposition of the center becomes more difficult and slower. The Ag_6 octahedra rearrange to form FCC-Ag lattice with an associated reduction in volume. These FCC-Ag nanoparticles are abundant in stacking faults (Figure 5d). This agrees with the structure model illustrated in Figures 3a and 4c. The transformation from the AgNH to FCC-Ag increases the CN of atoms in the lattice. However, the stacking of the close-packed planes is disordered. The metastability of the AgNHs further proves the above-proposed structure model of the AgNHs.

UV–vis Spectroscopy. Our investigations on the unique crystal structure of the AgNHs suggest that the organic–inorganic interaction is essential to the polyol process. We also measured the optical properties of AgNHs (Figure 6). The UV–vis spectrum of the AgNHs shows a broad peak in the

(21) Hirsh, P.; Howie, A.; Nicholson, R.; Parshley, D. W.; Welan, M. J. *Electron Microscopy of Thin Crystals*, revised edition; Krieger Publishing Co.: Huntington, 1977.

wavelength range of 300–600 nm, similar to the spectrum of FCC-Ag nano-octahedra of similar size.[13] Many fine features can be well resolved in the spectrum (Figure 6a), consistent with the complex shape. Both experimental and theoretical studies have proved that these fine features correspond to multiple localized surface plasmon resonance (LSPR) modes. Although the AgNHs have a very different crystal structure from that of FCC-Ag, it seems LSPR is also prominent as in nanostructured FCC-Ag.

SERS Activity. The Rhodamine-6G (R6G) molecule was used to test the SERS response. Figure 6b shows the R6G@glass sample which did not yield any characteristic peaks, while the R6G@AgNHs sample exhibited many characteristic Raman peaks. Therefore, the AgNHs act as an SERS-active substrate for chemical sensing and can be used as imaging agents in chemical detection. Both the UV–vis and the SERS results suggest that surface plasmons exist in AgNHs; i.e., there are collective oscillations of the conducting electrons in the AgNHs. The origin of the plasmon mode is not clear now; further investigations are needed.

Conclusions

In summary, we have synthesized a new Ag nanocrystal using the polyol process, AgNHs, which have a faceted concave shape with sharp tips. The AgNHs are single crystals with an FCC lattice (lattice constant 9.6193 Å) and consist of an Ag_6 octahedra skeleton stabilized by organic capping molecules. Each AgNH has six branches along the ⟨100⟩ directions and a sharp tip of four {111} facets. The AgNHs are metastable under electron beam irradiation, decaying to FCC-Ag nanoparticles with abundant stacking faults, probably due to removal of the capping molecules during irradiation. The study of the structure of the AgNHs offers further understanding of the organic–inorganic interaction involved in the polyol process. The template effect of the capping molecules on the growth of these well-defined nanocrystals operates on the atomic scale. The AgNHs also show remarkable optical properties and are an active substrate for SERS spectroscopy.

Acknowledgment. This work was supported by National 973 Project of China, National Natural Science Foundation of China, and National Center for Nano-Science and Technology of China. The authors thank Lewys Jones for revising the manuscript.

Supporting Information Available: High-resolution SEM images of an AgNH viewed from large different angles (Figure S1). This information is available free of charge via the Internet at http://pubs.acs.org.

CM702480A